J. Min. Metall. Sect. B-Metall. 50 (2) B (2014) 171 - 176

Journal of Mining and Metallurgy,
Section B: Metallurgy

Letter to Editor

CALCULATION OF TERNARY Si-Fe-Al PHASE EQUILIBRIUM IN VACUUM DISTILLATION BY MOLECULAR INTERACTION VOLUME MODEL

K. Liu [b,c], J.J. Wu [a,b,c*], W.H. Ma [a,b,c], B. Yang [a,b], X. Yang [b,c], L.X. Kong [b], X.F. Zeng [b,c], Y.N. Dai [a,b,c]

[a] State Key Laboratory of Complex Nonferrous Metal Resources Cleaning Utilization in Yunnan Province, Kunming University of Science and Technology, Kunming, P.R. China
[b] The National Engineering Laboratory for Vacuum Metallurgy, Faculty of Metallurgical and Energy Engineering, Kunming University of Science and Technology, Kunming, China
[c] Engineering Research Center for Silicon Metallurgy and Silicon Materials of Yunnan Provincial Universities, Kunming University of Science and Technology, Kunming, P.R. China

(Received 08 May 2014; accepted 23 October 2014)

Abstract

The vacuum distillation of aluminum from Si-Fe-Al ternary alloy with high content of Al is studied by a molecular interaction volume model (MIVM) in this paper. The vapor-liquid phase equilibrium of the Si-Fe-Al system in vacuum distillation has been calculated using only the properties of pure components and the activity coefficients. A significant advantage of the model lies in its ability to predict the thermodynamic properties of liquid alloys using only binary infinite dilution activity coefficients. The thermodynamic activities and activity coefficients of components of the related Si-Fe, Si-Al and Fe-Al binary and the Si-Fe-Al ternary alloy systems are calculated based on the MIVM. The computational activity values are presented graphically, and evaluated with the reported experiment data in the literature, which shows that the prediction effect of the proposed model is of stability and reliability.

Keywords: Molecular interaction volume model; Phase equilibrium; Si-Fe-Al alloy; Vacuum distillation

1. Introduction

The production of primary (new) aluminum is the largest in volume in the nonferrous metal industry. The current industrial production of aluminum from alumina is based on the electrochemical Hall-Heroult process, which has the drawbacks of high-greenhouse gas emissions and large energy consumption [1]. For about half a century, there have been sustained attempts and considerable efforts to produce aluminum from alumina by the alternative process of the carbothermic reduction of alumina [2,3]. Despite the process has been studied extensively and made some headway, it remains to be a formidable technical challenge. In a latest study [4], the production of Al-Si alloys had been studied by the vacuum carbothermal reduction of bauxite tailings containing mainly Al_2O_3, SiO_2 and Fe_2O_3 in a graphite furnace at pressures down to 10^{-9} bar and temperatures up to 2273K, resulting in the formation of an Si-Fe-Al alloy with high content of Al, as well as carbides, elementary Al, and Si. In order to acquire successful the aluminum, the separation of Si-Fe-Al alloy becomes an important step. Over past decades, vacuum metallurgy has been studied and successfully used in refining and separating of various crude metals by Dai [5] and Ali [6], and the area of its application is being extended rapidly.

Vacuum distillation is an effective method to acquire the volatile impurities Al from Si-Fe-Al alloy. Vacuum metallurgy has many advantages, such as high metal recovery, short flow sheet and good environmental protection etc., which can eliminate the disadvantages of traditional metallurgical processes. However, the absence of thermodynamic properties of Si-Fe-Al liquid alloys is difficult for understanding the process metallurgy. In order to obtain the thermodynamic properties of multi-component liquid alloys, the experiments are necessary and reliable. However, not enough data could be collected in those systems only by experiments without a large number of persons and time. Therefore, a unique economic and effective method to predict the behaviors by theory or by thermodynamic models depending on less experimental data is required. The MIVM [7] was derived from the statistical thermodynamics, more details were available in literature, which is of better stability and reliability to predict the thermodynamic properties and calculate the phase equilibrium of binary and multicomponent alloy systems in vacuum distillation [8-10].

The purpose of this work is to calculate phase

---

* *Corresponding author: dragon_wu213@126.com*

DOI:10.2298/JMMB140508021L

equilibrium of Si-Fe-Al alloy in vacuum distillation based on the MIVM. The predicted results will provide an important instructive significance for both experimental and practical vacuum distillation of Si-Fe-Al alloy. Meanwhile, the present work will provide effective and convenient model and principle for the separation and distribution of components of multicomponent alloy in vacuum distillation.

2. Verification of MIVM effectiveness

According to MIVM [7], the molar excess Gibbs energy G_m^E of the liquid binary alloy *i-j* is expressed as Eq. (1):

$$\frac{G_m^E}{RT} = x_i \ln\left(\frac{V_{mi}}{x_iV_{mi}+x_jV_{mj}B_{ji}}\right) + x_j \ln\left(\frac{V_{mj}}{x_jV_{mj}+x_iV_{mi}B_{ij}}\right) - \frac{x_ix_j}{2}\left(\frac{Z_iB_{ji}\ln B_{ji}}{x_i+x_jB_{ji}} + \frac{Z_jB_{ij}\ln B_{ij}}{x_j+x_iB_{ij}}\right) \tag{1}$$

as well as the activity coefficients of component *i* and *j* are expressed as Eq. (2) and Eq. (3), respectively.

$$\ln\gamma_i = \ln\left(\frac{V_{mi}}{x_iV_{mi}+x_jV_{mj}B_{ji}}\right) + x_j\left(\frac{V_{mj}B_{ji}}{x_iV_{mi}+x_jV_{mj}B_{ji}} - \frac{V_{mi}B_{ij}}{x_jV_{mj}+x_iV_{mi}B_{ij}}\right) - \frac{x_j^2}{2}\left(\frac{Z_iB_{ji}^2\ln B_{ji}}{(x_i+x_jB_{ji})^2} + \frac{Z_jB_{ij}\ln B_{ij}}{(x_j+x_iB_{ij})^2}\right) \tag{2}$$

$$\ln\gamma_j = \ln\left(\frac{V_{mj}}{x_jV_{mj}+x_iV_{mi}B_{ij}}\right) - x_i\left(\frac{V_{mj}B_{ji}}{x_iV_{mi}+x_jV_{mj}B_{ji}} - \frac{V_{mi}B_{ij}}{x_jV_{mj}+x_iV_{mi}B_{ij}}\right) - \frac{x_i^2}{2}\left(\frac{Z_jB_{ij}^2\ln B_{ij}}{(x_j+x_iB_{ij})^2} + \frac{Z_iB_{ji}\ln B_{ji}}{(x_i+x_jB_{ji})^2}\right) \tag{3}$$

Extending Eq. (1) to a multi-component alloy, its molar excess Gibbs energy can be expressed as Eq. (4)

$$\frac{G_m^E}{RT} = \sum_{i=1}^{n} x_i \ln\left(\frac{V_{mi}}{\sum_{j=1}^{n} x_jV_{mj}B_{ji}}\right) - \frac{1}{2}\sum_{i=1}^{n}\left(\frac{\sum_{j=1}^{n} x_jB_{ji}\ln B_{ji}}{\sum_{k=1}^{n} x_kB_{ki}}\right) \tag{4}$$

and the expression of activity coefficient of any component *i* is Eq. (5)

$$\ln\gamma_i = 1 + \ln\frac{V_{mi}}{\sum_{j=1}^{n} x_jV_{mj}B_{ji}} - \sum_{k=1}^{n}\frac{x_kV_{mi}B_{ik}}{\sum_{j=1}^{n} x_jV_{mj}B_{jk}} - \frac{1}{2}\left[\frac{Z_i\sum_{j=1}^{n} x_jB_{ji}\ln B_{ji}}{\sum_{l=1}^{n} x_lB_{li}} + \sum_{j=1}^{n}\frac{Z_jx_jB_{ij}}{\sum_{l=1}^{n} x_lB_{lj}} \times \left(\ln B_{ij} - \frac{\sum_{t=1}^{n} x_tB_{tj}\ln B_{tj}}{\sum_{l=1}^{n} x_lB_{lj}}\right)\right] \tag{5}$$

Where Z_i is the first coordination number. x_i, x_j and x_k are the molar fractions. The pair-potential energy interaction parameters B_{ij} and B_{ji} are defined as Eq. (6), respectively.

$$B_{ij} = \exp\left[-\left(\frac{\varepsilon_{ij}-\varepsilon_{jj}}{kT}\right)\right], \quad B_{ji} = \exp\left[-\left(\frac{\varepsilon_{ji}-\varepsilon_{ii}}{kT}\right)\right] \tag{6}$$

Where ε_{ii}, ε_{jj} and ε_{ij} are the pair-potential energies of *i-i*, *j-j* and *i-j*, respectively. $\varepsilon_{ij} = \varepsilon_{ji}$, and k is the Boltzmann constant.

For a binary system *i-j*, when x_i or x_j approaches zero, the infinite dilution activity coefficients γ_i^∞ and γ_j^∞ are deduced as Eq. (7) and Eq. (8), respectively.

$$\ln\gamma_i^\infty = 1 - \ln\left(\frac{V_{mj}B_{ji}}{V_{mi}}\right) - \frac{V_{mi}B_{ij}}{V_{mj}} - \frac{1}{2}\left(Z_i\ln B_{ji} + Z_jB_{ij}\ln B_{ij}\right) \tag{7}$$

$$\ln\gamma_j^\infty = 1 - \ln\left(\frac{V_{mi}B_{ij}}{V_{mj}}\right) - \frac{V_{mj}B_{ji}}{V_{mi}} - \frac{1}{2}\left(Z_j\ln B_{ij} + Z_iB_{ji}\ln B_{ji}\right) \tag{8}$$

Based on the infinite dilution activity coefficients γ_i^∞, γ_j^∞ of the binary liquid alloys and the value of the related parameters of their components, the required binary parameters B_{ij} and B_{ji} can be obtained from Eqs. (7) and (8) by using the Newton-Raphson methodology. Meanwhile, the values of B_{ij} and B_{ji} at other temperature can be obtained from Eq. (6) in which the pair-potential energy interaction parameters $-(\varepsilon_{ji}-\varepsilon_{ii})/k$ and $-(\varepsilon_{ij}-\varepsilon_{jj})/k$ may be assumed to be independent of temperature while the values of B_{ij} and B_{ji} at given temperature are known. The related parameters of the pure metals [11, 12] are shown in Table 1, the coordination number Z_i of liquid metals was available in document [13], the required binary parameters B_{ij} and B_{ji}, and the infinite dilution activity coefficients of the binary liquid alloy [14, 15] are respectively shown in Table 2.

Next, allowing the Si-Fe-Al ternary alloy to be the 1-2-3 system, the activity coefficient of the component 1 of the system can be written from Eq. (5).

$$\ln\gamma_1 = 1 + \ln\left(\frac{V_{m1}}{x_1V_{m1}+x_2V_{m2}B_{21}+x_3V_{m3}B_{31}}\right) - \frac{x_1V_{m1}}{x_1V_{m1}+x_2V_{m2}B_{21}+x_3V_{m3}B_{31}} - \frac{x_2V_{m1}B_{12}}{x_1V_{m1}B_{12}+x_2V_{m2}+x_3V_{m3}B_{32}} - \frac{x_3V_{m1}B_{13}}{x_1V_{m1}B_{13}+x_2V_{m2}B_{23}+x_3V_{m3}} - \frac{1}{2} \times \left(\frac{Z_1\left(x_2B_{21}+x_3B_{31}\right)\left(x_2B_{21}\ln B_{21}+x_3B_{31}\ln B_{31}\right)}{\left(x_1+x_2B_{21}+x_3B_{31}\right)^2}\right) + \frac{Z_2x_2B_{12}\left[\left(x_2+x_3B_{32}\right)\ln B_{12} - x_3B_{32}\ln B_{32}\right]}{\left(x_1B_{12}+x_2+x_3B_{32}\right)^2} + \frac{Z_3x_3B_{13}\left[\left(x_2B_{23}+x_3\right)\ln B_{13} - x_2B_{23}\ln B_{23}\right]}{\left(x_1B_{13}+x_2B_{23}+x_3\right)^2} \tag{9}$$

***Table 1**. The related parameters of the components Si, Fe and Al*

i	V_{mi} (cm^3/mol)	ΔH_{mi} (kJ/mol)	σ_i ($\times 10^{-8}$ cm)	d_{covi} ($\times 10^{-8}$ cm)
Si	11.1[1+1.4× 10−^{4}(T−1687)]	50.63	2.64	2.25
Fe	7.94[1+1.3× 10^{-4}(T−1808.15)]	13.77	2.46	2.34
Al	11.3[1+1.5× 10^{-4}(T−933.52)]	10.46	2.86	2.36

Substituting the corresponding parameters B_{ij} and B_{ji} into Eqs. (2) and (3), the activities of components in Si-Al, Si-Fe and Fe-Al binary alloy is obtained and shown in Figure 1. The results show that the calculated activities are in reasonable agreement with the experimental data [14, 15]. It is confirmed that the prediction of activities in the Si-Al, Si-Fe and Fe-Al binary alloy based on the present study is reasonable and reliable.

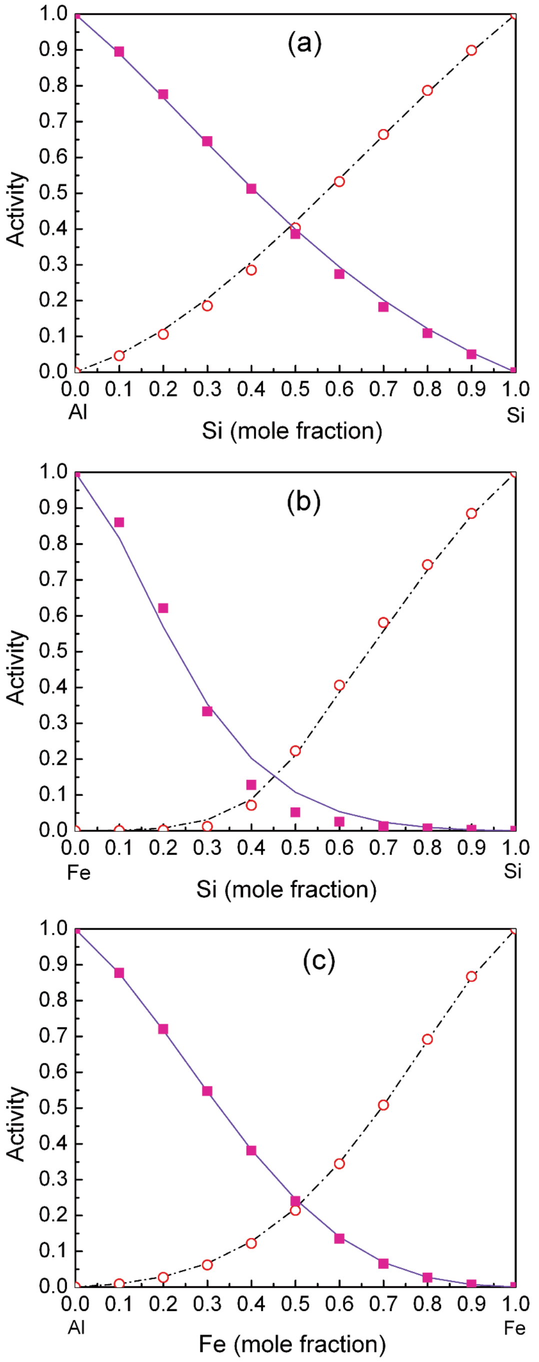

Figure 1. *Comparison of the predicted activities of MIVM (lines) with experimental data [14,15] (symbols) of alloy systems (a) Si-Al at 1700 K, (b) Si-Fe at 1873 K, (c) Fe-Al at 1900 K.*

Table 2*. The values of* γ_i^∞ *and* γ_j^∞*,* B_{ij} *and* B_{ji} *of the related binary alloys i-j at the required temperatures*

i-j	*T* /*K*	γ_i^∞	γ_j^∞	B_{ij}	B_{ji}	Z_i	Z_j
Si-Fe[15]	1873	0.00132	0.0162	1.7619	1.2079	5.8478	9.4905
Si-Al[14]	1700	0.416	0.495	1.2697	0.8708	6.1566	8.1525
Fe-Al[14]	1900	0.054	0.034	1.2611	1.3008	9.4477	7.8875

The activities of components Si-Fe-Al [16-19] system were chosen to check the validity of Eq. (9) since the data is well known to be reliable. Substituting the corresponding parameters B_{ji} and B_{ij} into Eq. (9), the activities of components in Si-Fe-Al ternary melt are obtained and compared with the Al experimental data at 1900K by Bedon et al. [16] and the calculated data using CALPHAD method at 1373K by Du and Liu et al. [17-19]. As shown in Figure 2., the reference state is pure liquid Al at the same temperature. It can be seen from Fig.2a and Fig.2b that the predicted values are in good agreement with the experimental and calculated values. It is

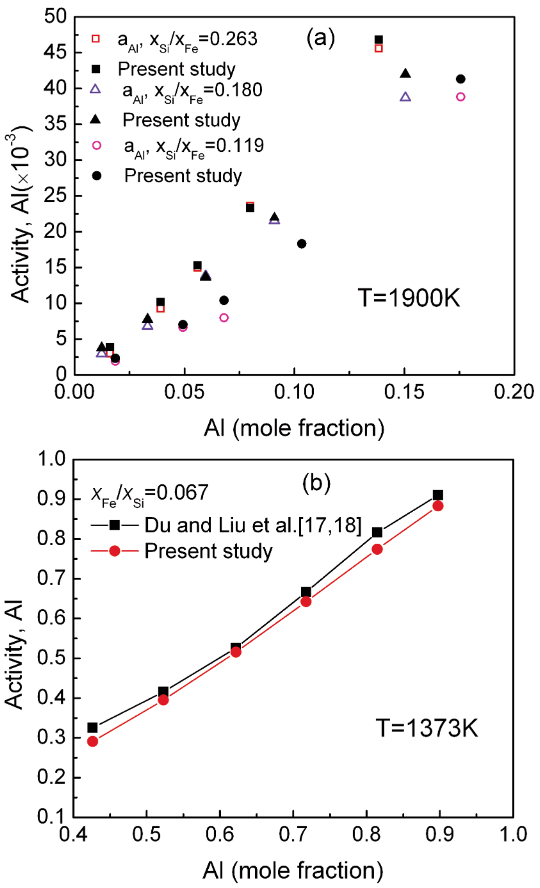

Figure 2. *(a) Al activities at 1900K according to the present model compared with experimental data by Bedon et al. [16], (b) Al activities at 1373K according to the present model compared with the optimized data by Du and Liu et al. [17,18].*

confirmed that the prediction of activities in the Si-Fe-Al ternary melt based on the present study is reasonable and reliable.

3. Method

3.1 Separation coefficient

According to thermodynamic equilibrium theory, Dai et al.[5] deduced the separation coefficient (β), which can be used to determine whether two components can be separated from each other by vacuum distillation and the separating degree of different elements in binary and multi-component alloys. The separation coefficient of component was presented as Eq. (10):

$$\beta = (\gamma_i / \gamma_j) \cdot (p_i^* / p_j^*) \tag{10}$$

Where γ_i and γ_j are activity coefficients of i and j components, respectively. P_i* and P_j* are the saturated vapor pressures of pure substances i and j, respectively. It is workable to the separation of components i and j when $\beta > 1$ or $\beta < 1$ but not when $\beta = 1$. The vapor pressures of pure substances Si, Fe and Al at required temperatures are shown in Table 3 [5].

***Table 3**. The saturated vapor pressure of components of the Si-Fe-Al system at required temperatures.*

T /K	1273	1373	1473	1573	1673	1773	1873
P^*_{Si} /Pa	5.34 $\times 10^{-6}$	8.03 $\times 10^{-5}$	8.34 $\times 10^{-4}$	6.41 $\times 10^{-3}$	3.85 $\times 10^{-2}$	1.89 $\times 10^{-1}$	7.81 $\times 10^{-1}$
P^*_{Al} /Pa	2.97 $\times 10^{-2}$	2.38 $\times 10^{-1}$	1.43 $\times 10^{0}$	6.84 $\times 10^{0}$	2.69 $\times 10^{1}$	9.07 $\times 10^{1}$	2.67 $\times 10^{2}$
P^*_{Fe} /Pa	9.31 $\times 10^{-5}$	1.13 $\times 10^{-3}$	9.78 $\times 10^{-3}$	6.38 $\times 10^{-2}$	3.31 $\times 10^{-1}$	1.42 $\times 10^{0}$	5.19 $\times 10^{0}$

3.2 Phase equilibrium of vacuum distillation

The vapor-liquid phase equilibrium diagram between vapor phase and liquid phase was investigated which can be used to predict the products' composition quantitatively and the distribution of components of i-j-k ternary alloy during the vacuum distillation. When the two phases are equilibrium, the mass fraction, $\omega_{i,\mathrm{g}}$, in vapor phase is related the vapor densities of these three components. We get Eq. (12).

$$\omega_{i,g} = \frac{\rho_i}{\rho_i + \rho_j + \rho_k} = \frac{1}{1 + \left(\frac{\rho_j}{\rho_i} + \frac{\rho_k}{\rho_i} \right)} \tag{12}$$

Where ρ_i , ρ_j and ρ_k are the vapor densities of component i, j and k, respectively, and $\rho_j/\rho_i = \omega_{j,\mathrm{l}}/\beta\omega_{i,\mathrm{l}}$, $\rho_k/\rho_i = \omega_{k,\mathrm{l}}/\beta\omega_{i,\mathrm{l}}$. The mass fractions, $\omega_{i,\mathrm{g}}$, in vapor phase are expressed as Eq. (13).

$$\omega_{i,g} = \left[1 + \frac{\omega_{j,l}}{\beta \cdot \omega_{i,l}} + \frac{\omega_{k,l}}{\beta \omega_{i,l}} \right]^{-1} = \left[1 + \left(\frac{\omega_{j,l}}{\omega_{i,l}} \right) \cdot \left(\frac{\gamma_j}{\gamma_i} \right) \cdot \left(\frac{p_j^*}{p_i^*} \right) + \left(\frac{\omega_{k,l}}{\omega_{i,l}} \right) \cdot \left(\frac{\gamma_k}{\gamma_i} \right) \cdot \left(\frac{p_k^*}{p_i^*} \right) \right] \tag{13}$$

The relationship between $\omega_{i,\mathrm{g}}$ and $\omega_{i,\mathrm{l}}$ are calculated by γ_i, p_i* and a series of $\omega_{j,\mathrm{l}}/\omega_{i,\mathrm{l}}$, $\omega_{k,\mathrm{l}}/\omega_{i,\mathrm{l}}$ at required temperatures.

4. Results and Discussion

4.1 Activities of components of the liquid Si–Fe–Al ternary alloy

As illustrated in Figure 1 and Figure 2, the prediction effect of the activities of components of Si-Fe-Al ternary alloy is of better stability and reliability based on the MIVM, so we substitute the corresponding parameters B_{ji} and B_{ij} and some parameters of pure metals into Eq. (9), the activities of components of the Si-Fe-Al ternary alloy can be predicted, as shown in Table 4.

***Table 4**. The predicted values of activities of components of the liquid Si–Fe–Al alloy in the temperature range of 1273-1873 K.*

x_{Si}	x_{Fe}	x_{Al}	a_{Si}	a_{Fe}	a_{Al}
T= 1273K					
0.1	0.4	0.5	0.1263	0.0669	0.1644
0.2	0.35	0.45	0.2353	0.0563	0.1562
0.3	0.3	0.4	0.3347	0.0468	0.1466
0.4	0.25	0.35	0.4291	0.0381	0.1354
0.5	0.2	0.3	0.5213	0.0299	0.1222
0.6	0.15	0.25	0.6132	0.0221	0.1071
0.7	0.1	0.2	0.7057	0.0145	0.0897
0.8	0.05	0.15	0.7994	0.0072	0.0703
0.9	0.025	0.075	0.8998	0.004	0.0338
T= 1373K					
0.1	0.4	0.5	0.1263	0.0795	0.1858
0.2	0.35	0.45	0.2325	0.0675	0.1756
0.3	0.3	0.4	0.3291	0.0568	0.1639
0.4	0.25	0.35	0.4219	0.0466	0.1502
0.5	0.2	0.3	0.514	0.0369	0.1344
0.6	0.15	0.25	0.6069	0.0274	0.1164
0.7	0.1	0.2	0.7013	0.0181	0.0962
0.8	0.05	0.15	0.7973	0.0089	0.0741
0.9	0.025	0.075	0.8992	0.0048	0.0354
T= 1473K					
0.1	0.4	0.5	0.1376	0.0938	0.2058
0.2	0.35	0.45	0.2384	0.0817	0.1943
0.3	0.3	0.4	0.3274	0.0702	0.1814
0.4	0.25	0.35	0.4147	0.0586	0.1661
0.5	0.2	0.3	0.5045	0.0468	0.1479
0.6	0.15	0.25	0.5979	0.0349	0.1269
0.7	0.1	0.2	0.6949	0.0229	0.1034
0.8	0.05	0.15	0.7944	0.0112	0.0782
0.9	0.025	0.075	0.8983	0.0059	0.037

table continuous on next page

table continuous

T=1573K					
0.1	0.4	0.5	0.1228	0.1062	0.2256
0.2	0.35	0.45	0.224	0.0921	0.2104
0.3	0.3	0.4	0.3173	0.0787	0.1938
0.4	0.25	0.35	0.4089	0.0655	0.1752
0.5	0.2	0.3	0.5018	0.0522	0.1544
0.6	0.15	0.25	0.5972	0.0389	0.1313
0.7	0.1	0.2	0.695	0.0256	0.1065
0.8	0.05	0.15	0.7946	0.0126	0.0803
0.9	0.025	0.075	0.8984	0.0066	0.038
T=1673K					
0.1	0.4	0.5	0.1037	0.1189	0.2434
0.2	0.35	0.45	0.2045	0.1021	0.2234
0.3	0.3	0.4	0.3035	0.0861	0.2023
0.4	0.25	0.35	0.4019	0.0706	0.1802
0.5	0.2	0.3	0.5001	0.0557	0.157
0.6	0.15	0.25	0.5985	0.0412	0.1327
0.7	0.1	0.2	0.6972	0.0271	0.1074
0.8	0.05	0.15	0.796	0.0134	0.0814
0.9	0.025	0.075	0.8989	0.0071	0.0387
T=1773K					
0.1	0.4	0.5	0.0996	0.132	0.2619
0.2	0.35	0.45	0.1984	0.1136	0.2391
0.3	0.3	0.4	0.2972	0.0959	0.2152
0.4	0.25	0.35	0.3962	0.0787	0.1904
0.5	0.2	0.3	0.4956	0.062	0.1648
0.6	0.15	0.25	0.5953	0.0458	0.1384
0.7	0.1	0.2	0.6953	0.0301	0.1113
0.8	0.05	0.15	0.7952	0.0148	0.0838
0.9	0.025	0.075	0.8987	0.0078	0.0398
T=1873K					
0.1	0.4	0.5	0.0954	0.1448	0.2802
0.2	0.35	0.45	0.1926	0.1247	0.2547
0.3	0.3	0.4	0.2912	0.1052	0.2281
0.4	0.25	0.35	0.391	0.0862	0.2007
0.5	0.2	0.3	0.4915	0.0679	0.1726
0.6	0.15	0.25	0.5925	0.0501	0.1441
0.7	0.1	0.2	0.6936	0.0328	0.1152
0.8	0.05	0.15	0.7945	0.0161	0.0862
0.9	0.025	0.075	0.8985	0.0085	0.0407

4.2 The separation of Al from Si-Fe-Al ternary alloy

Assume that the other impurity elements content in Si-Fe-Al ternary alloy are rarely and their evaporation don't affect the evaporation of Al. The comparison of saturated vapor pressure values of components at the same temperature can be used as a rough guide in determining which one should exhibit preferential evaporation. It can be seen from Table 3 that the saturated vapor pressure of Al is larger than three orders of magnitude to that of Fe and four orders of magnitude to that of Si at 1373K, and the saturated vapor pressure of Fe and Si are approximate at the same temperature. Therefore, Al will evaporate easily into vapor phase from Si-Fe-Al alloy and Si and Fe will tend altogether to remain in the residual phase during the vacuum distillation. However, it also can be seen from Table 3 that the saturated vapor pressure of Al is just larger than about 90 times to that of Fe at 1673K. Then, Si and Fe will evaporate partly into the vapor phase and condense on the cooling pan.

4.3 Phase equilibrium of ternary Si-Fe-Al alloy in vacuum distillation

As we have mentioned, the saturated vapor pressure difference in Si, Fe and Al can only be used as a rough guide for evaluating the possibility of separation of alloys by vacuum distillation, which could not be used to precisely predict the distribution of components of alloys. This study, therefore, will focus on the vapor–liquid phase equilibrium of ternary Si-Fe-Al alloy in vacuum distillation. According to the Table 4, we can acquire easily the activity coefficients γ_{Si}, γ_{Fe} and γ_{Al}. Then, substituting the activity coefficients γ_{Si}, $\gamma_{Fe,}$ γ_{Al} and P^*_{Si}, P^*_{Fe}, P^*_{Al} and a series of $\omega_{Fe,l}/\omega_{Al,l}$, $\omega_{Si,l}/\omega_{Al,l}$ at certain temperatures into Eq. (13), the vapor-liquid phase equilibrium of Si-Fe-Al ternary alloy at the different temperatures can be easily calculated as shown in Figure 3.

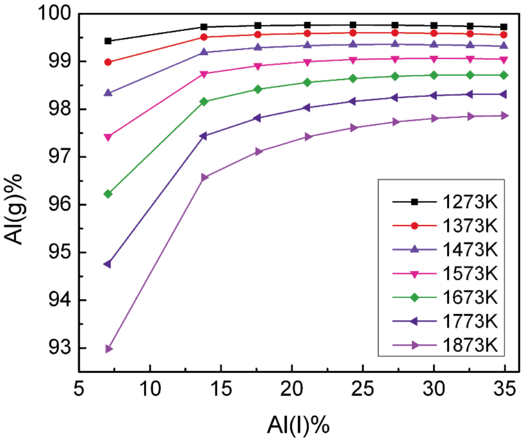

Figure 3. *Vapor–liquid equilibrium composition of Si-Fe-Al ternary system at the different temperatures*

It can be seen from Fig. 3 that when the content of Al in liquid phase is not less than 13% during the vacuum distillation, the content of Al in vapor phase decreases gradually with the temperature increasing. For example, when the content of Al in the liquid phase is 24.304 %, it is 99.762 % in vapor phase at

1273 K, and when the content of Al in the liquid phase is 24.304 %, it is 99.039 % in vapor phase at 1573 K. However, when the content of Al in liquid phase is less than 13%, the content of Al in vapor phase decreases observably and marks turning points at 13.809%. For example, when the content of Al in liquid phase is 17.61%, Al in vapor phase is 98.911 % at 1573 K, and when the content of Al in the liquid phase is 7.052 %, it is 97.425 % in vapor phase at 1573 K, it decreases 1.486 % in the vapor phase. In other words, the content of Si and Fe that evaporates into the vapor phase will increase 1.486 %. This behavior indicates that Si and Fe will evaporate partly into the vapor phase when the content of Al in liquid phase is less than 13% and the amount of Si and Fe increases observably with the increasing temperature, which will decrease the separation effect and influence the purity of production. Therefore, the lower temperature is beneficial to acquire successful the Al from Si-Fe-Al alloy. When the temperature is 1273 K, the content of Al in the liquid phase is 7.052 %, it is 99.428 % in vapor phase, and the content of Al in the liquid phase is 13.809 %, it is 99.769 % in vapor phase, the content of Si and Fe reached 0.231% in the vapor phase, which indicates that the purity of Al from Si-Fe-Al alloy after primary vacuum distillation is low, and multiple vacuum distillation is necessary. The predicted results will provide an important instructive significance for both experimental and practical vacuum distillation to acquire successful the Al from Si-Fe-Al alloy.

5. Conclusions

The vapor-liquid phase equilibrium of the Si-Fe-Al alloy in vacuum distillation have been calculated using only the properties of pure components and the activity coefficients, the results show that the content of Al in the liquid phase is 7.052 %, it is 99.428 % in vapor phase, and the content of Al in the liquid phase is 13.809 %, it is 99.769 % in vapor phase at 1273 K.The purity of Al from Si-Fe-Al alloy after primary vacuum distillation is not high enough, and multiple vacuum distillation is necessary. A significant advantage of the MIVM model lies in its ability to predict the thermodynamic properties of binary and multi-component liquid alloys using only binary infinite activity coefficients. Additionally, the study provides a rigorous model for calculating the vapor-liquid phase equilibrium which can explain the relation among materials, conditions of operation and quality of product in vacuum distillation.

Acknowledgments

The authors are grateful for financial support from the Natural Science Foundation of China (No. 51104080 and 51334002), the Natural Science Foundation of Yunnan Province (2014FB124), and the Program for Innovative Research Team in University of Ministry of Education of China(Grant No. IRT1250).

References

[1] Martin Halmann, Aldo Steinfeld, Michael Epstein and Irina Vishnevetsky, Mineral Processing and Extractive Metallurgy Review, 35 (2014) 126–135.

[2] Yuan H B, Yang B and Xu B Q, Transactions of Nonferrous Metals Society of China (in English), 20 (2010) 1505-1510.

[3] YuebinFeng, Bin Yang and Yongnian Dai, Transactions of Nonferrous Metals Society of China (in English), 22 (2012) 215-221.

[4] Yang D, Feng N X, Wang Y W and Wu X L, Transactions of Nonferrous Metals Society of China (in English), 20 (2010) 147–152.

[5] Dai Y N and Yang B, Vacuum metallurgy for Non-ferrous metals and materials. Metallurgical Industry Press, Beijing, 2000 (in Chinese).

[6] S.T. Ali, K. Srinivas Rao and C. Laxman, Separation and Purification Technology, 85 (2012) 178-182.

[7] Tao D P, Thermochimica Acta, 363 (2000) 105-113.

[8] Tao D P, Yang B and Li D F, Fluid Phase Equilibria, 193 (2002) 167-177.

[9] Yang H W, Yang B, and Xu B Q, Vacuum, 86 (2012) 1296-1299.

[10] Y.Y. Sun and M. Song, J. Min. Metall. Sect. B-Metall. 48 (1) B (2012) 45-51.

[11] T. Iida and R.I.L.Guthrie, The Physical Properties of Liquid Metals, Clarendon Press, Oxford, United Kingdom, 1988, 19-46.

[12] R.C. Evans, An Introduction to Crystal Chemistry, Cambridge University Press, London, 1976, 86.

[13] Tao D P, Metall. Mater. Trans. A, 36 (2005) 3495-3497.

[14] B. Predel and Landolt-Bornstein, Group IV: Physical Chemistry, vol. 12, Springer, Berlin, Heidelberg, New York, 2006.

[15] R. Hultgren, P.D Dessi, D.T. Hawkins, M. Geiser, and K.K. Kelley, Selected Values of the Thermodynamic Properties of Binary Alloys, ASM, Metals Park, OH, 1973

[16] P. Bedon, I. Ansara and P. Desre, Mem. Sci. Rev. Metall., 66 (1969), 907-913.

[17] DuY, J. Clements Schuster and Liu Z K et al., Intermetallics, 16 (2008), 554-570.

[18] Liu Z K, Y. Austin Chang, Metall. Mater. Trans. A, 30 (1999) 1081-1095.

[19] Z. Zovko Brodarac, N. Dolić, F. Unkić , J. Min. Metall. Sect. B-Metall. 50 (1) B (2014) 53-60.